Astron. Astrophys. 346, L21–L24 (1999)

ASTRONOMY AND ASTROPHYSICS

LETTER

Letter to the Editor

Identification of absorbing galaxies towards the QSO J2233–606 in the Hubble Deep Field South⋆

Laurence Tresse[1,2,8], **Michel Dennefeld**[1,3], **Patrick Petitjean**[1,4], **Stefano Cristiani**[5,6], **and Simon White**[7]

[1] Institut d'Astrophysique de Paris – CNRS, 98bis Boulevard Arago, F-75014 Paris, France
[2] Istituto di Radioastronomia del CNR, Via Gobetti, 101, I-40129 Bologna, Italy
[3] Université Pierre et Marie Curie, Paris, France
[4] DAEC – Observatoire de Paris, 5 Place Jules Janssen, F-92295 Meudon, France
[5] European Southern Observatory, Karl-Schwarzschild-Strasse 2, D-85748 Garching bei München, Germany
[6] Dipartimento di Astronomia, vicolo dell'Osservatorio 5, I-35122 Padova, Italy
[7] Max-Planck-Institut für Astrophysik, D-85740 Garching, Germany
[8] Laboratoire d'Astonomie Spatiale, B.P. 8, F-13376 Marseille Cedex 12, France

Received 8 December 1998 / Accepted 10 May 1999

Abstract. We present spectroscopic observations of galaxies lying within $1'$ of QSO J2233–606 in the Hubble Deep Field South (HDF-S). Several are found to be coincident in redshift with absorption-line systems seen in the HST J2233–606 spectrum. We detect a new $z_{\rm em} = 1.336$ QSO with $I = 20.8$ at a projected angular separation of $44.5''$ (or $\rho = 200h^{-1}$ kpc; $q_0 = 0.5$) from J2233–606. This QSO pair is an ideal target for QSO environment studies. Indeed, strong H I Lyα and Lyβ absorptions are seen at $z_{\rm abs} = 1.3367$ in the J2233–606 spectrum. The bright spiral galaxy (J2233378–603324), projected at $4.7''$ from J2233–606, is at $z = 0.570$ (thus $\rho = 18h^{-1}$ kpc). Absorption is seen in the Lyman series at the same redshift but the weakness of the Lyman break implies $N({\rm H\,I}) < 10^{17}$ cm^{-2}.

Key words: galaxies: halos – galaxies: ISM – galaxies: quasars: absorption lines – galaxies: quasars: individual: J2233–606

1. Introduction

Recently, a second HST deep field has been observed in the southern hemisphere (HDF-S; Williams et al. 1999, in preparation). The STIS field was chosen to contain the QSO J2233–606 ($z_{\rm em} = 2.238$, $B = 17.5$; Boyle 1997). Both deep imaging of the QSO field and spectroscopy of the QSO itself have been obtained (Gardner et al. 1999, Ferguson et al. 1999). Low- and high-dispersion spectra from ground-based telescopes are also already available (Outram et al. 1998, Savaglio 1998, Sealey et al. 1998). This set of data offers a unique opportunity to address important questions related to the connection between galaxies and QSO absorption lines, including the absorption cross-section of faint galaxies and the structure of the inter-galactic medium over the redshift range 1.2–2.2. Spectroscopy of the brightest galaxies in the full HDF-S, selected from our I-band ground-based image, has been performed on the ESO-NTT by a collaboration assembled under the auspices of a European Training and Mobility of Researchers (TMR) network. Here we comment on the galaxies closest to J2233–606 and discuss their possible relation with spectral features of J2233–606.

Sect. 2 briefly presents the target selection, observation and data reduction, with emphasis on objects close to J2233–606. In Sect. 3 we analyse their relevance to absorption lines in the J2233–606 spectrum. In Sect. 4 we draw our conclusions. Throughout the paper, we adopt $H_0 = 100h$ km s^{-1} Mpc^{-1} and $q_0 = 0.5$.

2. Data

2.1. Target selection, observation and data reduction

A 30mn equivalent I-band image centered on J2233–606 was obtained in the ESO Director's discretionary time with the EMMI-NTT red-imaging channel and made available to us for target selection. Photometric calibration has been done with standard stars from Landolt (1992) and the accuracy of the zero point is better than 0.1 magnitude. Source extraction and star-galaxy separation were performed with Sextractor (Bertin & Arnouts, 1996) resulting in a catalogue of 1159 objects with $I \leq 22.2$ complete at the 90% level. The US Naval Observatory catalogue was used as reference for the astrometry. This gives an accuracy close to $1''$ for absolute positions and about three times better for relative positions within the field. Multi-slit spectroscopy has been carried out with EMMI where about

Send offprint requests to: L. Tresse

⋆ Based on observations obtained with the NTT at the European Southern Observatory, La Silla, Chile under programs 61.A–0631 and 62.O–0363; and with the NASA/ESA Hubble Space Telescope by the Space Telescope Science Institute, which is operated by AURA, Inc., under NASA contract NAS 5–26555.

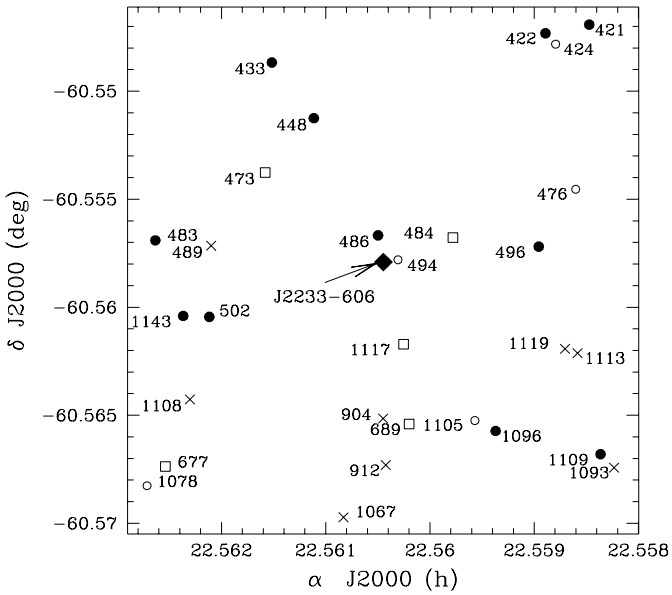

Fig. 1. Objects at $I \leq 22.2$ around J2233–606 (diamond symbol) with the running number of our photometric catalogue. North is at the top and East to the left. Objects with a compactness of more than 0.95, i.e. likely to be stars, are shown with crosses. For the remaining objects, circles represent the 16 objects at $I \leq 21.5$ of which 11 spectra have been obtained (filled circles). Squares represent fainter objects.

Table 1. Galaxies within a $1'$ radius of J2233-606 with the running number of our photometric catalogue (ID), the coordinates (α, δ), the I-band apparent magnitude (I), the heliocentric redshift (z), the angular separation (θ) to J2233–606, and the impact parameter (ρ/h).

ID	α (J2000) [°]	δ (J2000) [°]	I	z	θ [″]	ρ/h [kpc]
G422	338.38343	−60.5473	20.64	0.6465	56.8	220
Q433	338.42273	−60.5487	20.78	1.3360	44.5	190
G448	338.41668	−60.5513	19.55	0.5800	29.8	112
G483	338.43954	−60.5569	19.91	0.3302	58.4	170
G486	338.40752	−60.5567	20.32	0.5704	4.7	18
G496	338.38436	−60.5572	21.48	0.4148	39.9	130
G502	338.43177	−60.5604	18.57	0.2268	45.0	103
G1096	338.39056	−60.5657	20.79	0.4147	40.1	130
G1143	338.43553	−60.5604	21.29	0.066?	51.5	45

thirty objects can be observed simultaneously. We used slits of 1.02 or 1.34″ in width, leading to a spectral resolution of FWHM = 10.6 or 13.9 Å. The spectral range lies within 3900–10000 Å but its actual length depends on the location of the object within the mask. Reduction was done with standard techniques using an updated version of Multired under the IRAF reduction package. The residuals of the wavelength calibration fits have an r.m.s. of less than 0.7 Å, but the positioning of the objects relative to the slit was accurate to ∼0.3″, leading to wavelength uncertainties of order 3 Å. The accuracy in measuring the wavelengths of lines in the galaxy spectra is close to one tenth of the resolution element, i.e. 1. to 1.4 Å. Thus the redshift

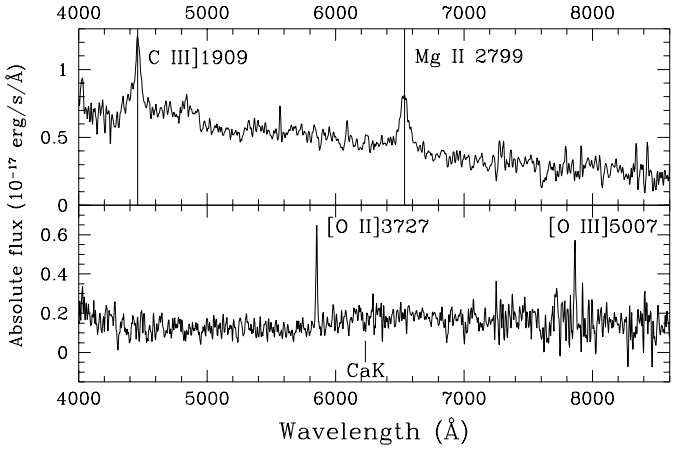

Fig. 2. Spectrum of Q433 (top) and G486 (bottom).

accuracy is mainly limited by the position of the galaxies within the slits, and our redshifts are accurate to about 0.001. Spectra were flux calibrated using standard stars from Stone & Baldwin (1984) with no attempt to correct here for aperture losses. Full details of observations of the complete sample, data reductions and measured parameters are in Dennefeld et al. (1999, in preparation).

2.2. Objects around J2233–606

Galaxies for which we have performed spectroscopy are shown by a filled circle in Fig. 1. Those galaxies lying within $1'$ of J2233–606 are listed in Table 1 two of which are of particular interest: Q433 (J2233415–603255) is another QSO, and G486 (J2233378–603324) is a spiral galaxy at only 4.7″ from J2233–606. Their spectra are displayed in Fig. 2. The redshift of Q433, $z = 1.336 \pm 0.001$, is determined from the broad Mg II λ2799 and C III] λ1909 emission lines. Also seen are the broad Fe II $\lambda\lambda$2400, 2600 complex, and the as yet unidentified broad feature around 2100 Å (see for instance Francis et al. 1991). The observed (V−I) spectral index is 0.5; using the corresponding spectral energy distribution gives $M(B) \simeq -21.5 + 5 \log h$. G486 is at $z = 0.570 \pm 0.001$ ([O II] λ3727, [O III] λ5007, CaK) and has a late-type spectrum consistent with its Sc morphology and the presence of numerous H II regions in the HST image. The observed (V−I) spectral index is 1.5, giving $M(B) \simeq -19.8 + 5 \log h$ (i.e. $L \sim L^*$).

3. Absorption lines in J2233–606

3.1. Q433 at $z_{\rm em} = 1.336$

We searched the HST spectrum for absorptions around $z = 1.336$. The wavelength ranges of H I Lyα together with C IV $\lambda\lambda$1548, 1550 and N V $\lambda\lambda$1238, 1242 around this redshift are shown in Fig. 3 on a relative velocity scale, v. Strong H I Lyα and Lyβ absorption lines are detected at $z_{\rm abs} = 1.3367$. The Lyβ line however is redshifted in a region of poor S/N below the Lyman break of the moderately optically thick system at $z \sim 1.9$ and is most certainly blended with Lyα absorption at a different

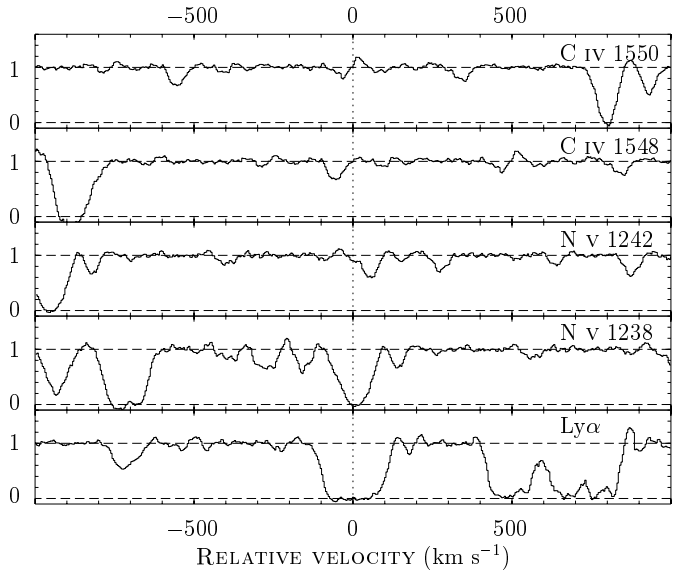

Fig. 3. Absorptions for the $z_{\rm abs} = 1.3367$ absorption-line system in the normalized J2233–606 spectrum. The Lyα line profile suggests a multi-component structure. From bottom to top, H I Lyα, N V 1238, N V 1242, C IV 1548, C IV 1550.

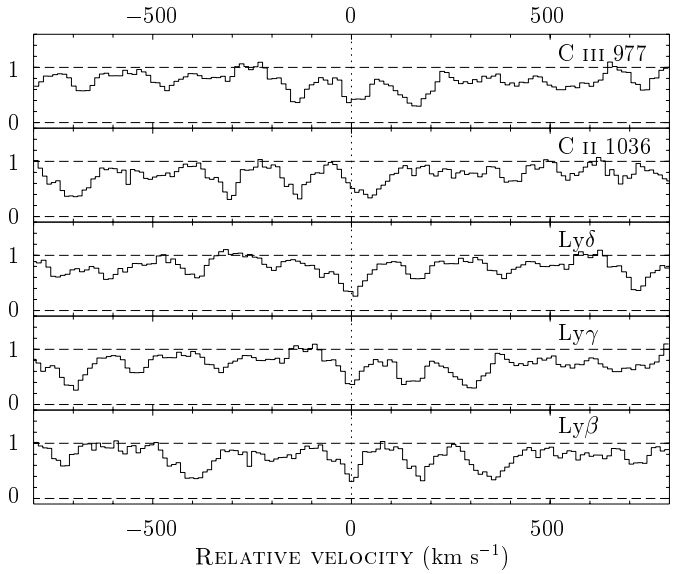

Fig. 4. Absorptions for the $z_{\rm abs} = 0.5705$ absorption-line system in the normalized J2233–606 spectrum. From bottom to top, H I Lyβ, Lyγ, Lyδ and C II 1036, C III 977.

redshift. More than one component are probably present since the continuum level at the bottom of Lyα goes to zero over about 150 km s^{-1} but neither damping wings nor an associated Lyman break are present. The total equivalent width of the Lyα line, $W_{\rm r} = 0.87$ Å, suggests a neutral hydrogen column density of at least $N({\rm H\,I}) \sim 10^{16}$ cm^{-2}. A one-component fit gives $N({\rm H\,I}) \sim 5\,10^{15}$ cm^{-2} and a Doppler parameter $b \sim 50$ km s^{-1}. The latter large value of b provides additional evidence for multiple structure. We tentatively fit the line with three components at $v \sim -51$, $+17$ and $+87$ km s^{-1} with $N({\rm H\,I}) \sim 2.5\,10^{14}$, $1.3\,10^{15}$, $5\,10^{13}$ cm^{-2} and $b \sim 38$, 33 and 25 km s^{-1} respectively. There might be a C IV λ1548 component at $v \sim -60$ km s^{-1} but with no obvious C IV λ1550 counterpart; the latter could be below the detection limit. N V λ1242 absorption could be present at $v \sim +55$ km s^{-1}. The N V λ1238 counterpart is unseen because it is blended with a strong Lyα line; and the associated C IV absorption is not detected. An absorption line is seen at the expected position of O VI λ1031 but with no obvious O VI λ1037 counterpart; the corresponding part of the spectrum has a poor S/N ratio however. The presence of metals in the cloud is thus questionable; better data in the optical range will help decide this issue.

The good correspondence between the redshift of Q433 and the Lyman absorption redshift in the J2233–606 spectrum ($\Delta z \sim 0.0007 \pm 0.001$, $\Delta v \sim 90 \pm 130$ km s^{-1}) might only be coincidence. The absorption could in fact be due to gas associated with an object in the QSO's immediate environment. We note that the number density of Lyα lines with $N({\rm H\,I}) > 10^{16}$ cm^{-2} is about 5 per unit redshift (Petitjean et al. 1993). Assuming no dependence on redshift, the probability that a randomly placed Lyα cloud with $N({\rm H\,I}) > 10^{16}$ cm^{-2} is observed within 200 km s^{-1} from the redshift of Q433 along the line of sight to J2233–606 is smaller than 0.01. This probability is not highly significant since it is an a-posteriori statistical argument. Note that Savaglio et al. (1999) have shown that the region spanning $z \sim 1.383$–1.460 has a low density of absorption lines with five lines detected when 16 are expected from the average density along the line of sight. This possible 'transverse proximity effect' is at odds with the presence of the strong line at the same redshift as Q433. A similar situation has been observed along the lines of sight to Q1026–0045A,B, two QSOs at $z_{\rm em} = 1.438$ and 1.520 respectively, with an angular separation of 36″, corresponding to an impact parameter of $\sim 150 h^{-1}$ kpc (Petitjean et al. 1998). A metal-poor associated system is seen at $z_{\rm abs} = 1.4420 \sim z_{\rm em}^{\rm A}$ along the line of sight to A, with a complex velocity profile. A strong Lyα absorption is detected along the line of sight to B, redshifted by only 300 km s^{-1} relative to the associated system in A.

Follow-up spectroscopic studies of the field will investigate whether this QSO/absorption association is a consequence of the presence of a gaseous disk, halo or other gaseous structure of radius larger than $200 h^{-1}$ kpc around Q433 or is due to a galaxy at a similar redshift to Q433.

3.2. G486 at $z_{\rm em} = 0.570$

The line of sight to J2233–606 passes through the disk (seen approximatively face-on) of a late-type spiral galaxy at an impact parameter of only $\sim 18 h^{-1}$ kpc. This is a situation where conspicuous metal absorptions, and perhaps damped H I Lyα, are expected. H I absorption associated with this galaxy is seen in the Lyman series (see Fig. 4) at $z_{\rm abs} = 0.570 \pm 0.01$. Uncertainties are too large to reliably estimate the column density from fitting the lines. However, the fit of the Lyman limit (912Å) gives $N({\rm H\,I}) \sim 10^{16.8}$ cm^{-2} (Outram, private communication). Be-

cause of the poor spectral resolution of the G140L spectrum, the presence of C III λ977 and C II λ1036 cannot be ruled out, and the C IV and Al III doublets are most certainly blended. There is no Fe II λ2600 absorption at λ4083.3 in the AAT spectrum (Outram et al. 1998) down to a 3σ limit $W_{\rm r}=0.03$ Å. The lack of Fe II absorption is consistent with a low H I column density. Note that Fe II λ2382 is lost in a strong Lyα complex.

It is well established that bright ($L_{\rm K} > 0.1\ L^*_{\rm K}$) galaxies within $40h^{-1}$ kpc from the line of sight to a QSO produce strong ($W_{\rm r} > 0.3$ Å) Mg II absorption (e.g. Bergeron & Boissé 1991, Steidel et al. 1994) whereas fainter galaxies with a similar range of impact parameters do not produce detectable metal-line absorptions (Steidel et al. 1997). In the present case, a weak absorption line at λ4390.66 is detected both in the AAT spectrum and in a spectrum recently obtained at ESO (V. D'Odorico et al., private communication). In the ESO spectrum, $W_{\rm obs}=0.18\pm0.04$ Å is observed. This line is probably Mg II λ2796 at $z=0.5701$. The limit on the corresponding weaker Mg II λ2803 line is consistent with the optically thin case. The Mg II absorption is quite weak for a galaxy with $L\sim L^*$ and such a small impact parameter: this is inconsistent with the correlation between the impact parameter and the strength of the absorption claimed by Lanzetta & Bowen (1990).

3.3. Other galaxies around J2233–606

A single component Mg II system is seen at $z_{\rm abs}=0.4143$ $b=7$ km s^{-1} and $\log N({\rm Mg\ II})=12.8$ (Outram et al. 1998). We observe two galaxies at a distance smaller than 40″ (or $130h^{-1}$ kpc) from J2233–606 at redshifts $z_{\rm em}\sim0.4147$ and 0.4148, (G1096 and G496 in Table 1), while a third one with $z_{\rm em}\sim0.4147$ (G1109) is slightly outside the 1′ radius ($\theta=63''$). The well-defined I-band selected CFRS redshift distribution gives 0.38±0.02 and 0.52±0.04 galaxies at $I\leq22$ by square arcmin in the respective redshift ranges [0.30–0.40] and [0.40–0.50] (see Lilly et al. 1995). Thus the three galaxies observed in a 0.0001 redshift range represent a density far in excess of the expected mean. This overdensity of galaxies at $z\sim0.4147$ suggests that other objects closer to the QSO are responsible for the absorption. A possible candidate is object G484 (see Fig. 1), at a distance of 18.2″, resolved in the HST image into an interacting pair of spirals.

For the other galaxies (G1143, G502, G483), no conspicuous Mg II is found, i.e. the $W_{\rm r}$ limit at 3σ is 0.10, 0.13 and 0.05 Å respectively at $z_{\rm abs}=0.066$, 0.227, 0.330. This is consistent with the halo radius-luminosity scaling-law found for Mg II absorption-selected galaxies (Bergeron & Boissé 1991, Steidel et al. 1994).

4. Conclusions

We have carried out spectroscopic observations of galaxies around J2233–606 and searched for associated absorption-line systems in its spectrum. We find the following.

(i) Q433 (J2233415–603255; $z=1.336$, $M(B)\simeq-21.5+5\log h$, $\rho=190h^{-1}$ kpc) is an ideal target for QSO environment studies. Strong H I Lyα and Lyβ absorptions are seen at $z_{\rm abs}=1.3367$ in the spectrum of J2233–606. The good redshift agreement might be coincidence; however a similar case has already been observed by Petitjean et al. (1998). Further investigations are needed to decide whether a group of galaxies associated with Q433 or a structure of radius larger than $200h^{-1}$ kpc around Q433 is responsible for the H I absorption.

(ii) The nearly face-on Sc spiral (J2233378–603324; $z=0.570$, $M(B)\simeq-19.8+5\log h$, $\rho\sim18h^{-1}$ kpc) is an excellent target for associated absorption-line system studies. We find absorption in the Lyman series. The associated Lyman limit, and the absence of Fe II in the J2233–606 spectrum are consistent with a H I column density of less than 10^{17} cm^{-2}. The Mg II absorption is weak for a galaxy with $L\sim L^*$ and such a small impact parameter; this is inconsistent with a tight correlation between impact parameter and absorption strength.

(iii) A Mg II absorption system is detected at $z_{\rm abs}=0.4143$ in the J2233–606 spectrum. At the same time, there is an overdensity of galaxies at $z\sim0.4147$, so other objects closer than 40″ to J2233-606 are expected at the same redshift. G484 ($I=21.5$) is a good candidate for being related to this absorption.

Acknowledgements. We thank P. Outram for his comments. This program has been conducted with partial support by the Training and Mobility of Researchers network under contract FMRX-CT96-0086: 'The Formation and Evolution of Galaxies'. LT acknowledges financial support by the same network.

References

Bergeron J., Boissé P., 1991, A&A 243, 344
Bertin E., Arnouts S., 1996, A&AS 117, 393
Boyle B.J., 1997, AAO Newsletter 83, 4
Francis P.J., Hewett P.C., Foltz C.B., et al., 1991, ApJ 373, 465
Landolt A.U., 1992, AJ 104, 340
Lanzetta K.M., Bowen D., 1990, ApJ 357, 321
Lilly S.J., Tresse L., Hammer F., et al., 1995, ApJ 455, 108
Outram P.J., Boyle B.J., Carswell R.F., et al., 1998, MNRAS submitted (astro-ph/9809404)
Petitjean P., Webb J.K., Rauch M., et al., 1993, MNRAS 262, 499
Petitjean P., Surdej J., Smette A., et al., 1998, A&A 334, L45
Savaglio S., 1998, AJ 116, 1055
Savaglio S., Ferguson H.C., Brown T.M., et al., 1999, ApJ submitted (astro-ph/9901022)
Sealey K.M., Drinkwater M.J., Webb J.K., 1998, ApJ 499, L135
Steidel C.C., Dickinson M., Persson S.E., 1994, ApJ 437, L75
Steidel C.C., Dickinson M., Meyer D.M., et al., 1997, ApJ 480, 568
Stone R.P.S., Baldwin J.A., 1984, MNRAS 204, 347